Criticality in creep experiments on cellular glass

C. Maes and A. Van Moffaert
Institute for Theoretical Physics, Katholieke Universiteit Leuven, Celestijnenlaan 200D, B-3001 Leuven, Belgium

H. Frederix and H. Strauven
Pittsburgh Corning Europe N. V., Albertkade 1, B-3980 Tessenderlo, Belgium

(Received 10 November 1997)

Creep experiments on cellular glass under a constant compressive load are monitored by acoustic emission. The statistical analysis of the acoustic signals emitted by the sample while stress is being internally redistributed shows that the distribution of amplitudes follows a power law, $N(A) \sim A^{-\beta}$, with $\beta = 2.0$ independent of the load. Similarly, the interarrival times between two recorded events are also distributed via a power law, $\tau^{-\gamma}$, where $\gamma = 1.3$. Finally, the distribution of the spatial distance between two consecutive events also shows scale invariance, $\rho(r) \sim r^{-\pi}$ with, under additional assumptions, $\pi = 1.6$. [S0163-1829(98)09909-3]

Since the introduction of the notion of self-organized criticality (SOC) by Bak, Tang, and Wiesenfeld[1] in 1987, a large number of publications has been devoted to the theoretical analysis of SOC models, their simulation, and their relevance for realistic situations. The study of sandpile models and of spring-block models, just to mention two major examples, has played an important role in clarifying the nature of the phenomenon. Not only is the concept of SOC thought useful as a general paradigm of spontaneously evolved criticality (possibly related to the ubiquity of fractals, $1/f$ temporal noise, self-similarity, . . .),[2] but it has also been able to shed new light on aspects of specific phenomena from sometimes distant fields. Nevertheless, studies of SOC phenomena in controlled (or real) (laboratory) experiments have remained more limited. One of the difficulties in associating SOC with real experiments is that this already implies a particular theoretical framework or interpretation of the observed phenomenon. Yet, it is by now not crystal clear what is and what is not to be called SOC, and what this concept could add to the understanding of an observed power-law behavior. We wish to avoid these controversies and to stick to the facts: we report on an experimentally observed power-law behavior for which the exponents are identical to those measured in other setups including computer simulations for models which are SOC thought.

The present article's purpose is to contribute further experimental evidence for scale invariance in microfracturing processes via the acoustic emission for the followup of creep in cellular glass. Similar questions are discussed in Refs. 3–8. In particular our observations provide evidence for the predictions by Zaitsev[9] that creep processes have to demonstrate power-law behavior. We thus have a laboratory realization of what has been called extremal dynamics. We strongly believe indeed that this evidence can be extended to other materials than those considered here. In fact it is surprisingly simple to observe critical phenomena in the response of construction materials to a constant compressive load. Via acoustic emission we have monitored the distribution of energy releases and of the time interval between emissions. In both cases we find a power law with exponents consistent with other SOC realizations obtained there via real measurements, theoretical predictions or computer simulations. Using earthquake terminology, we have concentrated on the so-called Gutenberg-Richter and Omori laws with, in addition, a measurement of the spatial distance between consecutive events. The observed exponents coincide with those found in Ref. 10 where the punctuated-equilibrium model of biological evolution (Ref. 18) is applied to earthquakes.

Generic scale invariance (within physical cutoffs) is mostly manifested in power-law distributions characterizing the dynamical response of the system's state to an external driving. The latter can take the form of strains or stresses applied to a material; in our case it is induced by applying a compressive load elastically deforming the body. This load is constant in time allowing the system to adjust to it, i.e., there is an infinite time scale separation between the external driving and the relaxation of the material. One should think of the system as composed of many locally connected interacting components. These components can be pictured as microscopic defects on the glass interface. Cellular glass is a large surface, containing a huge amount of microscopic defects. A defect starts to grow when its stress intensity in tension exceeds the static fatigue limit of glass. Below this threshold global reorganization of the glass surface is possible to diminish local stress intensity maxima. This is sometimes associated with the so-called glass surface fluidity by which small defects in glass can be self-restored chemically.[11,12] This restoration might influence neighboring defects or cells and it is not always totally efficient, giving rise to small microcracks in the material. As such the material can exist in a large number of different microscopic states that differ, e.g., in internal stresses or crack structures. The dynamics takes the material from one metastable (glass) state to the other while emitting energy. The result is an avalanche of reactions by which the material lets itself be heard by acoustic signals of varying amplitude (or energy). Energy diffusion on this fractal cellular substrate between regions containing defects are responsible for the distribution of the time interval between energy bursts. Obviously, when the compressive load is too large this mechanism fails altogether and the result is a macroscopic crack or defect in the exposed material.

The above mechanism shares properties of both so-called threshold and extremal dynamics. Due to the constant external force a complicated structure of local deformations can be expected. It is only when a critical tension (static fatigue limit) is exceeded that the self-restoration of microdefects is no longer effective (the threshold mechanism). The most deformed cells are obviously the first to undergo changes (the extremal mechanism). For example, the first energy bursts originate mainly from the center of the glass block as it is there where the initial deformations are most pronounced. The potential energy of the components is growing to a certain point after which it is released kinetically to neighboring components. The resulting deformations can in turn give rise to further bursts of energy release in ever more distant regions. It is this ''avalanche state'' that is monitored in our samples via acoustic emission methods. In the end a new mechanical equilibrium is found between the external stress and the internal forces (the acoustic emission signal dies out).

Note that we do not attempt here to provide a detailed microscopic description of the dynamics governing these complex materials. One of the major merits of the SOC paradigm is to account for certain universal macroscopic behavior irrespective of the details of the underlying microscopics as long as the latter can be viewed at least qualitatively as sharing essential ingredients with such prototype models as sandpiles,[1] stick-slip processes,[13,14] Burridge-Knopoff spring-block models,[15,16] extremal (or Robin Hood) models,[9,17,18] etc. This suggests that SOC dynamics can be observed from the scale of earthquakes to that of microfracturing processes and it is tempting to include also our system in the SOC family. But, obviously, the mere existence of power laws in our system cannot be sufficient for claiming SOC in any meaningful way. It is now well recognized that there are many other scenarios for power laws,[19] and competing theoretical frameworks as those concerning disordered first-order transitions[7,20] cannot be excluded.

Turning back to the avalanche state we have concentrated on two types of observations: the amplitude and the interarrival time of the bursts of energy release. In the SOC literature the names of Gutenberg-Richter and of Omori are associated with them. They refer to phenomenological laws, observed in a very specific context, whose universality and origin have been clarified using the notion of SOC. The Gutenberg-Richter law gives the distribution of energies released at any event, $N(E) \sim E^{-b}$. In 1956 (Ref. 21) it appeared with $b = 1.4 - 1.6$ as giving the number of observed earthquakes (in a certain region during a certain time) with energy E. Sornette *et al.*,[22] assuming frictional forces only between the components, obtained $b = 2$ via a simple mean-field-type argument. Taking into account both elastic compression and static friction Chen *et al.*[16] obtained $b = 1.5$. This is also the value of the exponent measured by Cannelli *et al.*[3] via acoustic emission associated to fracture processes in hydrogenated niobium and of that measured by Diodati *et al.*[23] for the ultrasonic emission from volcanic rocks. Petri *et al.*[4] measured the value $b = 1.3$ in the acoustic signals from laboratory samples subjected to an external uniaxial elastic stress. The Omori law[24] also appeared in earthquake statistics and gives the scaling for the distribution function of the time interval between two recorded events (two successive bursts) $N(\tau) \sim \tau^{-\gamma}$ with exponent $\gamma = 1$ obtained in the mean-field analysis of Sornette *et al.*[22] and in the simulations of Zapperi *et al.*,[7] $\gamma = 1.3$ in the simulation of Chen *et al.*,[16] and $\gamma = 1.2$ as measured by Diodati *et al.*[23] Vespignani *et al.*[5] measured an exponent $\gamma = 1.6$ but they have a rather large spreading in their measurements.

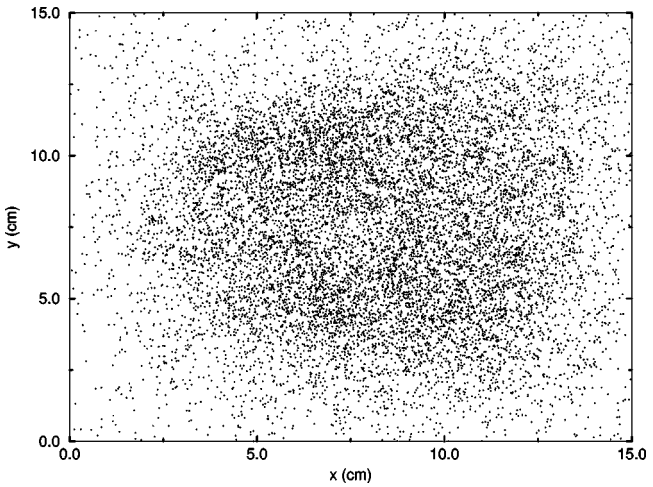

FIG. 1. Distribution of events projected on the xy plane (perpendicular to the applied stress) after a few minutes.

Our samples are $15 \times 15 \times 10\ \mathrm{cm}^3$ cellular glass blocks. One cell has a size of about 1 mm. Cellular glass is a closed cell foam with a soda-lime glass composition. The investigated type is Foamglas^{R}F with a density of 170 kg/m^3. It is used as a high mechanical strength insulation product. The average compressive strength is 1.7 N/mm^2. The samples are unidirectionally compressed on a hydraulic press. As capping, we used a 1mm thick Rhepanol rubber on the top and bottom faces. Resonant differential sensors (Dunegan: D150-M1) are fixed on the sample and are connected through preamplifiers on a digital Vallen AMS3 acoustic emission system. The frequency range is from 50 to 500 kHz with a variation in transfer of about 20 dB. Sound velocities of the order of 290 m/s are obtained in accordance with the known elasticity modulus (1500 N/mm^2) and the density. The samples are loaded up to a constant compressive stress. Localization plots show that the events are homogeneously distributed over the sample (Fig. 1) (no pre-existent macroscopic defects). In fact, initially most events originate from the center of the sample as it is there where the cells are most deformed (lower elasticity modulus). The material shows less than 1 dB acoustic damping in the scale of our sample. While initially we used four probes, located symmetrically around the sample in the plane orthogonal to the load, the data change very little when using only one probe.

The detected acoustic-emission (AE) signals are limited by the noise level. Only energy bursts with a maximum amplitude exceeding 30 dB are recordable. Two separate events arriving within 4 ms are not distinguished and registered as one event. After about 100 h the number of recorded events drops to almost zero. The total amount of recorded events is then of the order of 50 000. The average energy per event decreases in time but this is not due to acoustic damping or decreased sensor sensitivity. Finally, when a material that was exposed for a sufficiently long time to a certain constant load is put back under the hydraulic press, the emission of

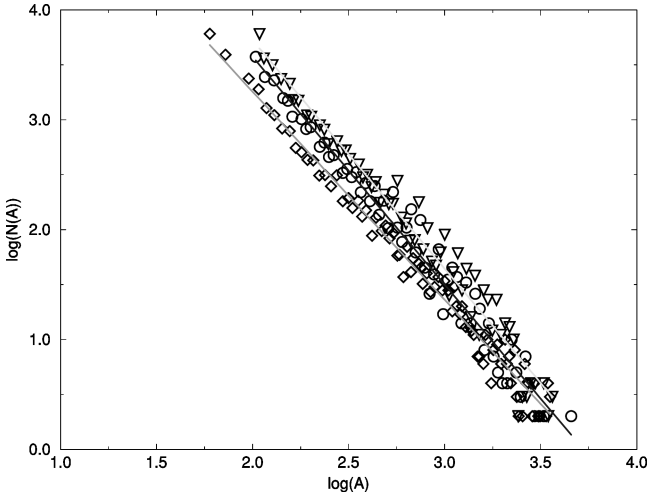

FIG. 2. The logarithm of the number of registered events with amplitude A is plotted versus the logarithm of A (in μV) for three different loads (diamonds, triangles, and circles). The experimental results can be fit by a line with slope -1.90, -2.10, and -2.08, respectively.

energy bursts only restarts when the load exceeds that previous load. This is known as the Kaiser effect and it is consistent with the above picture.

In Fig. 2 the amplitude distribution is shown for loads varying between 0.8 and 1.0 N/mm^2. For each load about six different samples were exposed to the same load. The amplitude distribution can be transformed in an energy distribution (the energy is proportional to the square of the amplitude) which can be fitted by the scaling law

$$N(E) \sim E^{-b},$$

$b = 1.5 \pm 0.1$ when averaged over the different loads. Since $A^2 \sim E$, $N(A) \sim A^{-\beta}$ with $\beta = 2b - 1$. Note that the number of decades over which this behavior is manifested is independent of the load. We thus find a Gutenberg-Richter behavior with the same exponent b as in Refs. 23,16.

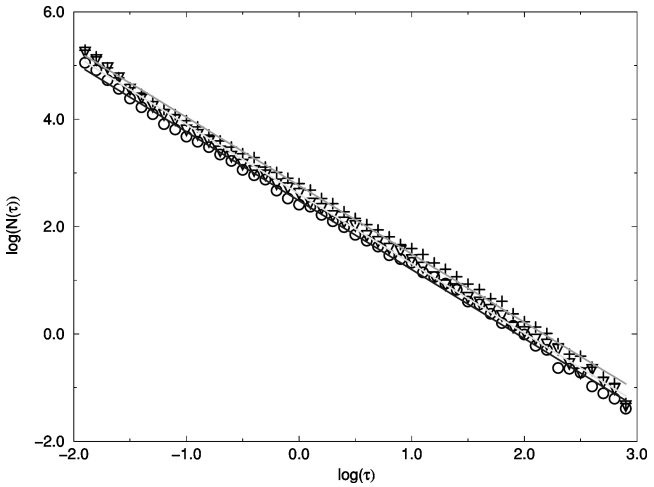

FIG. 3. The logarithm of the number of events registered with an interarrival time τ (in s) is plotted versus the logarithm of τ. This is done for three different loads (circles, triangles, and crosses). A linear fit of the experimental values gives slope -1.28, -1.29, and -1.27.

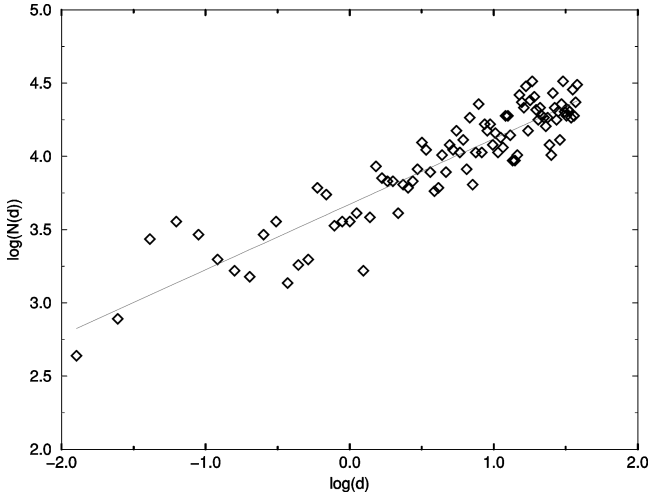

FIG. 4. Plot of the logarithm of the number of consecutive events at distance d versus the logarithm of d. This however is not the real (three-dimensional) distance but the distance ($d^2 = x^2 + y^2$) after projection on a plane perpendicular to the stress. The experimental results (diamonds) are compared with a linear fit with slope 0.4.

In Fig. 3 the Omori behavior is checked. In the same way we find for the interarrival time distribution the scaling

$$N(\tau) \sim \tau^{-\gamma},$$

$\gamma = 1.27 \pm 0.01$ in agreement with Ref. 23. When we increase the amplitude threshold, taking it from 40 to 45 dB and thereby throw away about 30% of the original data, we still find that this (new) Omori exponent is 1.27 ± 0.01. When we restrict ourselves to recording only the events within the first 10 h (and not, as previously, take all the events in the 100 h window), we still find the value of 1.28 ± 0.01 for the Omori exponent.

Figure 4 results from computing distances $d = \sqrt{x^2 + y^2}$ (see Fig. 1) between consecutive AE events. The power-law exponent must be corrected to obtain the distribution function. Assuming that in three dimensions this distribution scales like $p(r) \sim r^{-\pi}$ ($r = \sqrt{x^2 + y^2 + z^2}$, z is the vertical di-

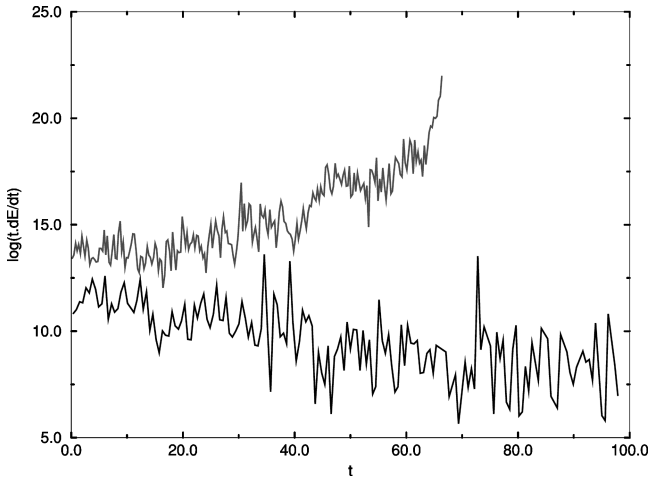

FIG. 5. Energy dissipation $t \cdot dE/dt$ versus time for large and small loads.

rection) we get $\pi = 1.6$. It is interesting to note that then $\pi = 2\gamma - 1$ relating via a (normal) diffusive scaling law the spatial exponent π to the Omori exponent γ.

An important question in material science and in geophysics is to identify precursors of macroscopic defects or shocks. In our case the question is to differentiate in the behavior of the material under compressive load according to whether or not a macroscopic crack will appear. We have always found that whenever the rate of energy dissipation is decreasing faster than $1/t$ (say in the first 20 h), then the sample does not break in the observed 1000 h (see Fig. 5). If the material survives the external load, the rate at which energy is dissipated is decreasing and can be fitted via $dE/dt = 1/te^{\alpha t}$ with $\alpha < 0$. If however the load becomes too high (above a critical strength) the system becomes unstable. In all those cases we found that now α is positive and increases with growing load. It would be interesting to understand how the $1/t$ failure criterium for the energy dissipation rate can be understood from a theoretical point of view or whether a similar behavior can be observed in simplified models. Precursors for rupture very similar to the upper curve of Fig. 5 have been studied before in Refs. 25 and 26.

Cracks propagate through solids subject to external strains or stresses. Their nature is controlled by instabilities at the smallest scale. While a detailed microscopic picture is lacking (see, e.g., the discussion in Ref. 27), SOC dynamics provide a qualitative explanation of the observed macroscopic behavior. The most striking aspect of the latter is the mere fact of observing discrete pulses of energy release governed as well in amplitude as in interarrival times and distances by power laws. Our experimental results give quantitative evidence in accord with other observed SOC phenomena, either simulated or measured.

This work was supported in part by the EC Grant No. CHRX-CT93-0411. C.M. and A.V.M. would like to thank the FWO Flanders for financial support.

[1] P. Bak, C. Tang, and K. Wiesenfeld, Phys. Rev. Lett. **59**, 381 (1987).
[2] P. Bak and M. Paczuski, Phys. World **6**(12), 39 (1993).
[3] G. Cannelli, R. Cantelli, and F. Cordero, Phys. Rev. Lett. **70**, 3923 (1993).
[4] A. Petri G. Paparo, A. Vespignani, A. Alippi, and M. Costantini, Phys. Rev. Lett. **73**, 3423 (1994).
[5] A. Vespignani, A. Petri, A. Alippi, and G. Paparo, Fractals **3**, 839 (1995).
[6] P. A. Houle and J. P. Sethna, Phys. Rev. E **54**, 278 (1996).
[7] S. Zapperi, P. Ray, H. Stanley, and A. Vespignani, Phys. Rev. Lett. **78**, 1408 (1997).
[8] G. Caldarelli, F. D. Di Tolla, and A. Petri, Phys. Rev. Lett. **77**, 2503 (1996).
[9] S. I. Zaitsev, Physica A **89**, 411 (1992).
[10] K. Ito, Phys. Rev. E **52**, 3232 (1995).
[11] D. Abriou, Y. Levillain, H. Arribart, and F. Creuzet, Verre **2**, 3 (1996).
[12] J. Zarzycki, *Glasses and the Vitreous State* (Cambridge University Press, Cambridge, 1991).
[13] J. M. Carlson and J. S. Langer, Phys. Rev. Lett. **62**, 2632 (1989).
[14] H. J. S. Feder and J. Feder, Phys. Rev. Lett. **66**, 2669 (1991).
[15] R. Burridge and L. Knopoff, Bull. Seismol. Soc. Am. **57**, 341 (1967).
[16] K. Chen, P. Bak, and S. P. Obukhov, Phys. Rev. A **43**, 625 (1991).
[17] M. Paczuski, P. Bak, and S. Maslov, Phys. Rev. Lett. **74**, 4253 (1995).
[18] P. Bak and K. Sneppen, Phys. Rev. Lett. **71**, 4083 (1993).
[19] D. Sornette, J. Phys. I **4**, 209 (1994).
[20] J. V. Andersen, D. Sornette, and K. Leung, Phys. Rev. Lett. **78**, 2140 (1997).
[21] G. Gutenberg and C. Richter, Ann. Geofis. **9**, 1 (1956).
[22] A. Sornette and D. Sornette, Europhys. Lett. **9**, 197 (1989).
[23] P. Diodati, F. Marchesoni, and S. Piazza, Phys. Rev. Lett. **67**, 2239 (1991).
[24] F. Omori, Rep. Earth. Inv. Comm. **2**, 103 (1894).
[25] J. C. Anifrani, C. Le Floc'h, D. Sornette, and B. Souillard, J. Phys. I **5**, 631 (1995).
[26] D. Sornette, Phys. Rep. (to be published).
[27] M. Marder and J. Fineberg, Phys. Today, **49**(9), 24 (1996).